Int J Adv Manuf Technol (2018) 95:811–823
https://doi.org/10.1007/s00170-017-1251-8

ORIGINAL ARTICLE

An embedded multi-sensor system on the rotating dynamometer for real-time condition monitoring in milling

Muhammad Rizal[1] · **Jaharah A. Ghani**[2] · **Mohd Zaki Nuawi**[2] · **Che Hassan Che Haron**[2]

Received: 15 May 2017 / Accepted: 24 October 2017 / Published online: 3 November 2017

Abstract The newly developed multi-sensor system for a milling process sensor system is capable of simultaneously measuring six channels of machining signals using a rotating tool incorporating a wireless system. Furthermore, the system can be used to measure the spindle torque, T_q; tool vibration in the z-axis, A_z; tool tip temperature, T_m and the three components of the cutting force. Cutting force signals are generated by using a cross-beam-legged transducer embedded in the standard milling tool holder. A mini accelerometer is placed under the force transducer, whereas a thermocouple is positioned under a cutting tool insert close to the cutting edge. All signals are collected and sent to the data logger system via an inductive wireless transmitter unit incorporated into the standard rotating tool holder. The calibration, verification and real experimental machining test results reveal that the sensor system is both suitable and reliable for measuring machining signals. The measured signals are found to be importantly related to changes in the flank wear state. Therefore, this system can be used for real-time tool condition monitoring in the milling process.

Keywords Multi-sensor system · Machining signal measurement · Cutting force · Torque · Vibration · Temperature · Wireless system

✉ Muhammad Rizal
muh.rizal@unsyiah.ac.id

[1] Department of Mechanical Engineering, Faculty of Engineering, Syiah Kuala University (UNSYIAH), 23111 Darussalam, Banda Aceh, Indonesia

[2] Department of Mechanical and Materials Engineering, Faculty of Engineering and Built Environment, Universiti Kebangsaan Malaysia, UKM, 43600 Bangi, Selangor, Malaysia

1 Introduction

Manufacturing industries are moving towards the adoption of fully automated systems, not only to control equipment but as an effective means of meeting current and future market demands. One of the principal issues in the automation of machining processes is the implementation of a reliable and efficient system to monitor tool conditions. Using such systems has reportedly increased productivity levels by 10 to 50%, and consequently increasing savings up to 40% [1]. The basic concept behind a tool condition monitoring system is in the acquisition of real-time information regarding the state of the cutting tool during machining operations. Any changes or alterations in the state of the cutting tool will cause different symptoms and information to result. Therefore, in detecting these symptoms, the sensor system is very important to enable the variety of signals generated during the machining process to be observed. These signals include the cutting force, torque, vibration, acoustic emission, sound pressure, temperature, and the current or spindle power [2, 3]. Hence, the development of a suitable and effective sensor system for a machining process monitoring system continues to be a major challenge.

The most popular signal in the milling process for a tool condition monitoring system is the cutting force [1–4]. Based on the literature, most researchers used the table dynamometer to measure the cutting force. However, it should be pointed out that a commercial dynamometer is deemed to be unsuitable for use in monitoring systems for industrial processes given the excessive costs involved. While previous researchers [5, 6] fabricated an alternate dynamometer based on a strain gauge, the use of this tool is limited to the laboratory environment due to the weaknesses in the geometry and dimensions of the workpiece to be cut. Furthermore, a table dynamometer has limited capability, including signal drift when measuring static forces [7]. Nevertheless, commercial

table dynamometers continue to be used for fundamental studies on machining research because they provide highly accurate cutting force readings.

Utilising a power or a current signal has been used to monitor the cutting tool in the milling process [8]. However, a power signal is strongly influenced by the viscous damping feed system and the friction of the mechanical system in milling machine components. The sound signal is also used by monitoring systems to measure the intensity of sound via a microphone [9]. However, such systems exhibit weaknesses when perceiving sound signals because they tend to capture and record all sounds, including noise, the sound of coolant flow, the noise of workshop environment and other parallel machining operations, which filter into the sensor. Vibration and acoustic emission signals can be detected directly by using a piezoelectric sensor placed on a workpiece [10]. However, the quality of the signal is often unstable as the distance between the cutting zone and the sensors are constantly changing during milling operations because of the relative movement of the tool holder in three axes during the cutting process. Furthermore, the cutting tool holder rotates such that the measurement becomes impossible when a sensor wire-based system is placed on it.

Therefore, a wireless system is possibly the only solution that can address the limitations of sensor systems, which are not able to be placed on the tool holder. Such a system would enable the sensor to be placed as close as possible to the cutting zone, even in the rotating tool holder used during the milling and drilling processes. In this way, the sensors used to measure temperature can be directly placed onto the cutting tool, thereby addressing limitations in vibration measurement associated with the effects regarding irregular and inconsistent distances from the cutting zone [11]. Previous studies have used a wireless system to acquire the machining signal. Suprock et al. [12] developed a wireless vibration sensor system for non-invasive integration into milling tool holders to detect the onset of regenerative chatter. Coz et al. [13] and Kerrigan et al. [14] proposed a temperature measurement system for rotating cutting tools where they incorporated a wireless transmitter unit into a tool holder, near to which a radio-frequency antenna was placed. Totis et al. [15] developed a rotating dynamometer capable of measuring individual cutting edge forces during face milling. The device was based on piezoelectric tri-axial force cells installed behind each cutting insert, where a wireless telemetry system transferred the signal. In a separate study, Ma et al. [16] proposed a wireless system for torque measurement in the milling process using a piezoelectric film attached to the tool shank.

Recently, several innovative rotating dynamometers have been developed such as by Rizal et al. [17], where they developed a rotating dynamometer using a cross-beam force transducer for measuring the cutting force in three directions. Qin et al. [18] proposed using a dynamometer to measure the axial force and torque in the milling process. Xie et al. [19] also developed a rotating dynamometer using capacitive sensors placed on the modified tool holder. However, these proposed systems only measured cutting force components. Furthermore, when these systems are used for condition monitoring via the multi-sensor to improve the precision, more equipment is often required to collect the data from the various sensors. As a result, the costs associated with the sensor system increase and the sensor wires become entangled in the machine zone.

This paper focuses on developing an embedded multi-sensor system on a rotating tool that is capable of simultaneously measuring torque, vibration, temperature, and three components of cutting force within a wireless environment. A rotating dynamometer for cutting force measurement was proposed in a previous study [17]; however, this system was limited to theoretical stress-strain analysis and a dynamic test. So, in this work, a mini accelerometer, thermocouple and strain gauges are integrated for torque measurement into a strain gauge-based rotating dynamometer.

2 Development of a multi-sensor system on the rotating tool

2.1 Measurement principle

When the milling cutter cuts the workpiece material, it will generate the cutting force, torque, vibration, and heat on the tool's edge. The cutting force components based on the rotating coordinate system are shown in Fig. 1. The main cutting

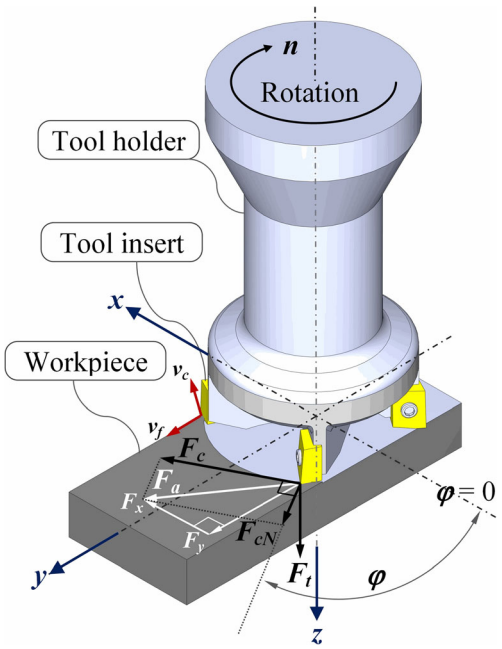

Fig. 1 Components of cutting force in face milling

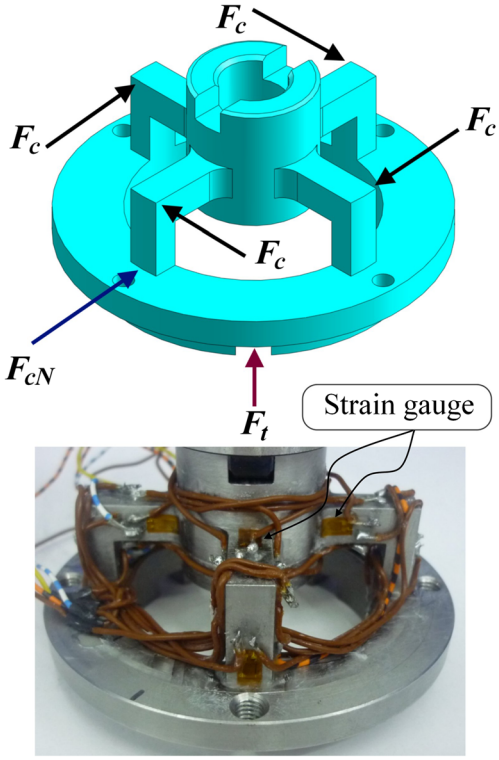

Fig. 2 Designed and constructed of force transducer

force, F_c, acts in the direction of the spindle rotation, n and the cutting speed, v_c. On the other hand, the perpendicular cutting force, F_{cN}, is in the direction towards the centre of the tool holder. The vertical interaction between the milling cutter and

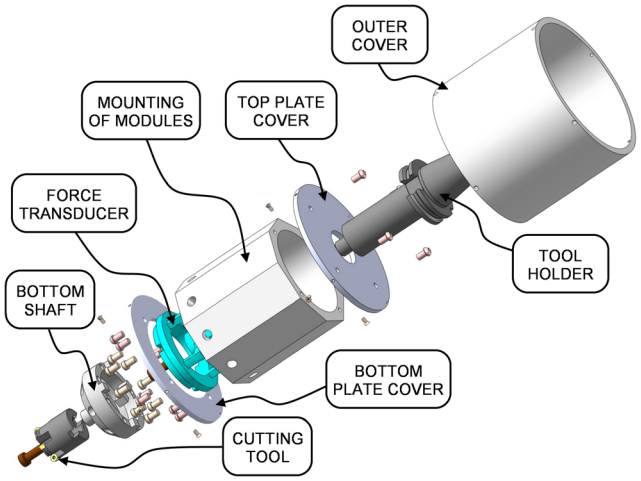

Fig. 4 Disassembled view of the sensor structure system

the workpiece causes a reactive force to occur regarding the thrust force, F_t. In the fixed coordinate system, the feed force, F_f, occurs when the tool holder moves forward of the workpiece. The relationship of the cutting force components in the rotating and fixed systems can be expressed by the following eqs. [17]:

$$F_c = F_f \cos\varphi + F_{fN} \sin\varphi \tag{1}$$

$$F_{cN} = F_f \cos\varphi + F_{fN} \cos\varphi \tag{2}$$

$$F_x = F_f \tag{3}$$

$$F_y = F_{fN} \tag{4}$$

Fig. 3 Positioning of strain gauges on the tool holder shaft for torque measurement

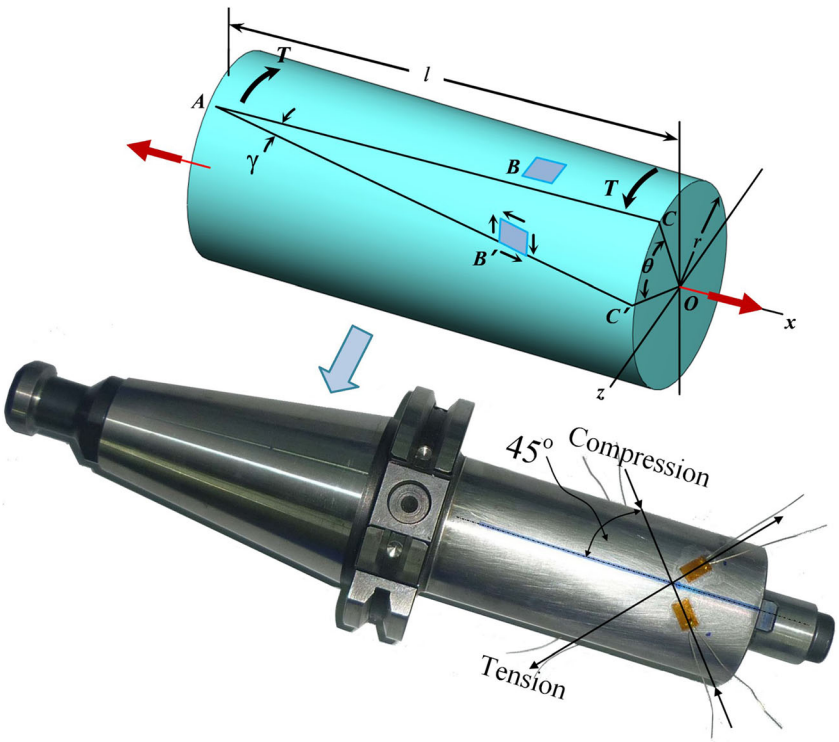

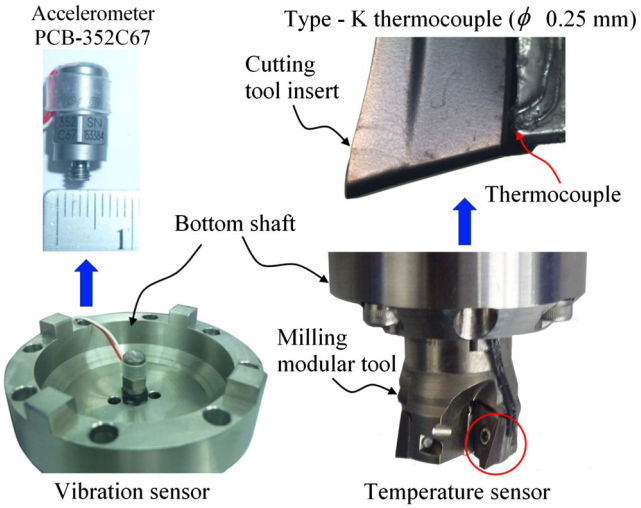

Fig. 5 Setup of vibration and temperature sensor

$$F_z = F_t \tag{5}$$

$$F_a = F_c^2 + F_{cN}^2 = F_x^2 + F_y^2 \tag{6}$$

In detecting the three components of the cutting force during milling, a force transducer was designed and constructed as shown in Fig. 2, which was used and discussed for the development of a rotating dynamometer in the previous study [17].

The rotation of the spindle milling machine will generate torque as the machine operates, which creates stress on the surface of the tool holder shaft. Torque can be detected using strain gauges mounted on the tool holder, as shown in Fig. 3. Given that stress caused by torque T occurs on the surface of the shaft, the maximum shear stress occurring on the surface of the round shaft can be written as

$$\tau = \frac{Tr}{J} \tag{7}$$

where J is the polar moment of inertia ($J = \pi d^4/32$ for the solid shaft), such that Eq. (7) becomes

$$\tau = \frac{16T}{\pi d^3} \tag{8}$$

Based on Hooke's law, the shear stress and shear strain are linear, such that

$$\tau = \gamma G \tag{9}$$

where G is the modulus of rigidity or shear modulus, and γ is a shear strain. By replacing the shear stress in Eq. (8), the torque can be obtained by applying Eq. (10):

$$T = \frac{\pi d^3 G}{16}\gamma \tag{10}$$

The torque is measured by attaching strain gauges (350 Ω) to a standard tool holder of the milling process. The tool holder material is 20CrMnTi (E = 225.5 GPa and v = 0.3) with a diameter shaft of 40 mm.

In fabricating the proposed multi-sensor system, an accelerometer and thermocouple were used to measure tool vibration and temperature. Figure 4 shows a modified structure that was designed and constructed to enable the placement of the sensor system on the tool holder in a wireless system environment. A single-axis PCB accelerometer was attached to the bottom of the shaft to detect vertical vibration (A_z). Meanwhile, a temperature sensor, which is a type-K thermocouple, was placed below the cutting tool insert, as shown in Fig. 5.

2.2 Instrumentation of the sensor system

The machining signals generated from an integrated multi-sensor system placed on a rotating tool holder are impossible to transmit (i.e. send) unless a wireless data transfer system is available. Figure 6 illustrates the circuit sensor system using a wireless telemetry system. KMT Telemetry GmbH manufactured this system, which can transmit voltage signals via the inductive principle. All modules of the sensor system were placed on the mounting material made of plastic. The system consisted of four modules for the strain gauge (MT32-

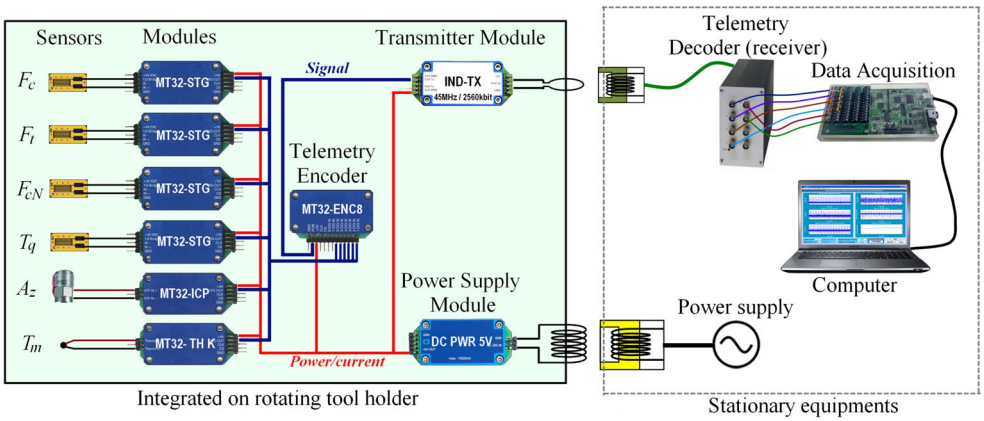

Fig. 6 Schematic diagram of a wireless telemetry system and its instrumentation on a rotating tool

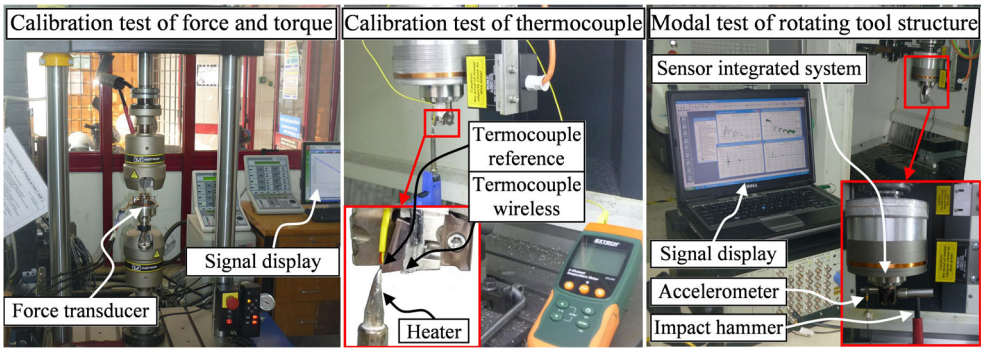

Fig. 7 Static and dynamic calibration test setup

STG) used to measure the main cutting force, F_c; the thrust force, F_t; the perpendicular cutting force, F_{cN} and the torque, T_q. The system also included one module for the accelerometer (MT32-ICP) and one module for the thermocouple sensor (MT32-TH K). The vibration sensor used a single-axis ceramic piezoelectric accelerometer (Model 352C67). The performance of the accelerometer can measure vibration with a maximum range of 491 m/s^2 and with an output sensitivity of 9.94 mV/(m/s^2).

In acquiring the temperature at the tool's edge during the milling process, a thermocouple (Omega CHAL-010-BW) was placed and embedded below the cutting tool insert. The sensor is a precision fine wire thermocouple with a diameter of 0.25 mm and is capable of measuring temperature up to 871 °C. Furthermore, to collect the signals from the six channels, an encoder MT32-ENC8 was used. Next, using a transmitter module MT32-IND-Tx-45 MHz-2560 k, the signals are transmitted within a frequency range of 45 MHz rating up to 2560 kb/s. The antenna coil is wrapped around the outer cover to transfer the data using the inductive transmitter. The sensor modules in this system were arranged in the mounting of the modules that were designed in a polygonal shape to avoid rotational imbalance of the tool holder. The modular cutting tool was aligned using a dial gauge until a maximum error of less than 8 μm was achieved.

A 5-V DC powered all the electronic modules and wireless systems. In the stationary system, a receiver or telemetry decoder consisting of eight channels (MT32-DEC8) and a data acquisition device (DT9836) were used. The voltage signal was the primary output from six channels and was processed using MATLAB software. The resonance frequency of the rotating dynamometer structure and the high-frequency noise of the device system were filtered off by applying a low-pass filter with a cut-off frequency at 450 Hz.

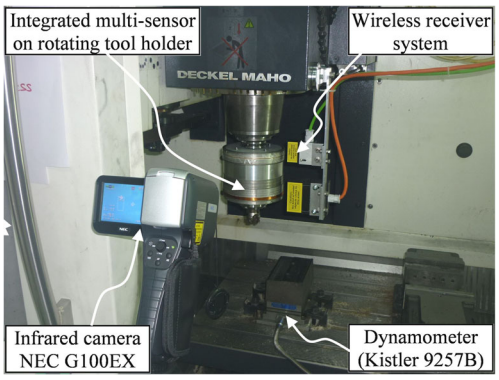

Fig. 8 Experimental setup for verification test

3 Experimental tests

3.1 Calibration test

In assessing the performance of a multi-sensor system integrated into a rotating tool, static calibration was used on the sensors to measure the main cutting force, F_c; thrust force, F_t; perpendicular cutting force, F_{cN}; torque, T_q and temperature, T_m. Figure 7 shows the calibration setup of the multi-sensor system. Static calibration for the cutting force and torque sensors was carried out on a servo-hydraulic machine (Instron 8874). The results of the calibration test of the rotating dynamometer were reported previously [17]. In this work, only the calibrated torque and temperature sensors are examined. The loading torque applied to the structure of the torque sensor ranged from 5 to 50 Nm, with a step increase of 5 Nm.

For the temperature sensor, the cutting tool tip was heated using electric heaters until reaching a temperature of approximately 200 °C according to a four-channel thermometer,

Table 1 Machining parameter for verification test

No. Exp.	Cutting speed, v_c (m/min)	Feed rate, f_z (mm/gigi)	Depth of cut, a_e (mm)
1	250	0.10	0.8
2	250	0.15	1.0
3	375	0.10	0.8
4	375	0.15	1.0
5	500	0.10	0.8
6	500	0.15	1.0

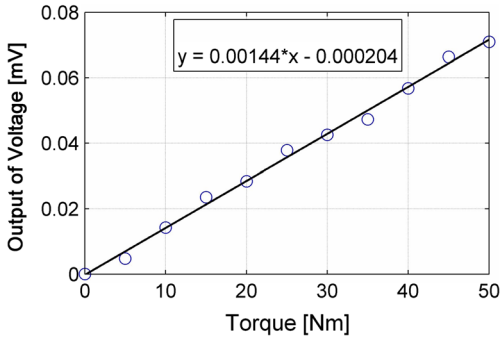

Fig. 9 Calibration curve of the torque sensor

Extech SDL200. Meanwhile, the temperature generated at the points was observed using a thermocouple placed below the cutting tool inserts. The temperature signal was recorded using a data acquisition card DT9836 via the wireless system, with a sampling of the data at a frequency of 1 kHz. An average of three readings from sensor data sampling was used to determine the sensitivity of all sensors. The vibration sensor exhibited high sensitivity due to the integration of the accelerometer sensor and calibration result reaching 9.94 mV/(m/s^2).

3.2 Verification test

After the calibration tests were conducted, the integrated rotating tool sensor system was ready to use in the actual milling process. A comparison test was conducted which was important to verify the performance of the developed sensor system. The cutting force and torque signals were obtained using the readings obtained from the wireless multi-sensor system and compared with the cutting forces and torque measured using a Kistler dynamometer 9257B. Figure 8 shows the experimental setup for the comparison test between the developed wireless multi-sensor system and commercial sensors. The cutting force was measured using a rotating force transducer with a coordinate-rotating system that generates readings on a flat surface, namely F_c and F_{cN}. The result differs from the cutting force that was measured using a table dynamometer which produces forces at fixed coordinates, for instance, F_x and F_y.

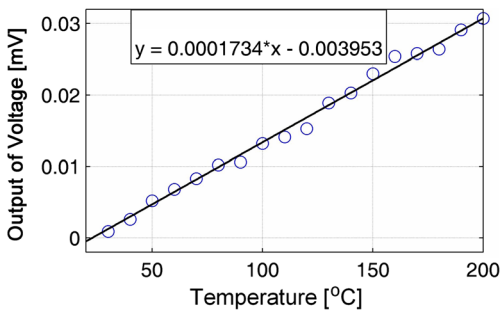

Fig. 10 Calibration curve of the temperature sensor

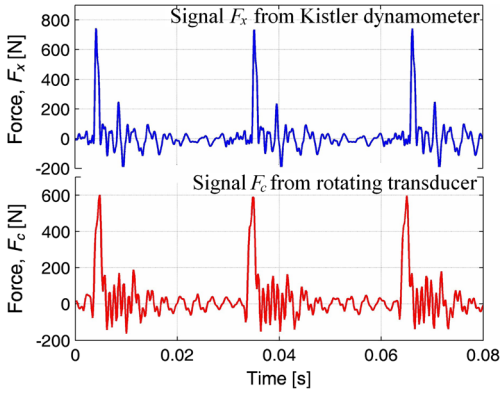

Fig. 11 Comparison of F_x and F_c forces when milling FCD700 at exp. set 1

However, the resultant active force (F_a) for the milling process will generate the same reading between the rotating transducer and the table dynamometer, as shown in Fig. 1 of Sect. 2.

The F_z force reading of the table dynamometer is the same as the F_t on the rotating transducer, which is caused by force generated in the same direction, i.e., parallel to the direction of the tool holder. While the torque signal is measured on the rotating sensor, the moment signal is measured in the z-axis using a table dynamometer, represented as M_z. The cutting force and torque were recorded using a data acquisition system, a charge amplifier Kistler 5070 for the table dynamometer and wireless devices for the developed multi-sensor system.

A set of experiments were conducted by end milling FCD700 ductile cast iron, as shown in Table 1. The axial depth of the cut is constant at 1 mm. The experiment used a tungsten carbide-coated tool with ACK300 grade on a CNC milling machine under dry conditions.

To evaluate the wireless system's performance in terms of vibration measurements, vibration signals will be detected when machining is performed using parameters in the experimental set 3: $v_c = 375$ m/min, $f_z = 0.1$ mm/tooth, $a_e = 0.8$ mm

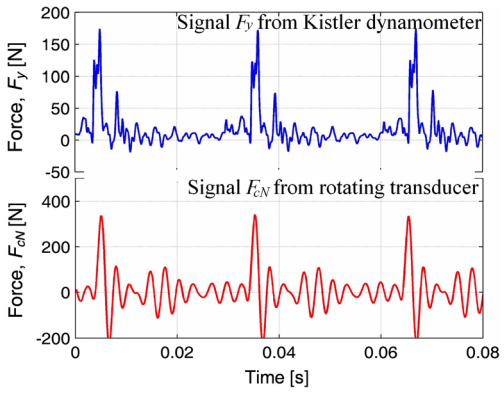

Fig. 12 Comparison of F_y and F_{cN} forces when milling FCD700 at exp. set 1

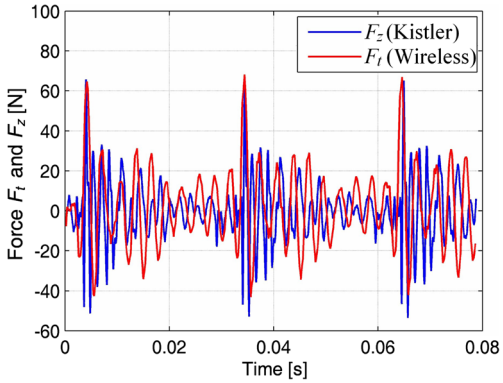

Fig. 13 Comparison of F_z and F_t forces when milling FCD700 at exp. set 1

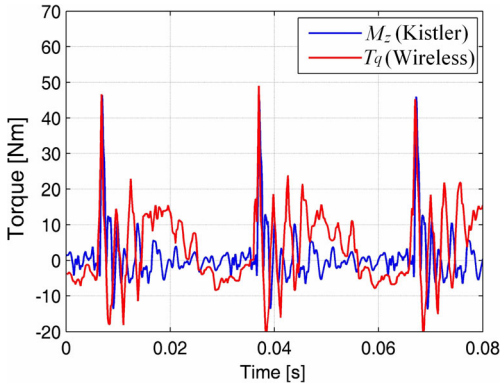

Fig. 15 Comparison of moments M_z and T_q when milling FCD700 in exp. set 1

and a_p = 1 mm. The other accelerometer is mounted on the spindle house of the milling machine. Signals were observed using the accelerometer Endevco model 751–100 and data acquisition device NI9234. An infrared camera NECG100EX was used to compare the temperature readings to assess the capability of the thermocouple sensor using a wireless system. The parameters used were included in experimental set 1: v_c = 250 m/min, f_z = 0.1 mm/tooth, a_e = 0.8 mm and a_p = 1 mm. The temperature signal sampling rate was 5 kHz for the data transmitted by the wireless system, and machining tests were conducted thrice to confirm the repeatability of the sensor readings.

3.3 Machining test for tool condition monitoring

These tests were designed to correlate the machining signals obtained from the wirelessly integrated multi-sensors on the rotating tools, such as the main cutting force, perpendicular cutting force, thrust force, torque, vibration and temperature, with the tool condition being the wear level. The machining tests were performed on a CNC milling machine (DMC 635 V eco) in dry cutting conditions of an end-milling operation. A coated tungsten carbide tool (Sumitomo AXMT170504PEER-G) with coated grade ACP200 is mounted on a standard modular of the cutting tool. The insert is a rectangular type, and nose radius is 0.4 mm, the thickness is 5.59 mm and width is 10.2 mm. Also, the clearance angle is 11°, and the length is 17.54 mm. A steel tool (AISI P20 + Ni) with a composition of 0.37% C, 0.30% Si, 1.40% Mn, 0.01% S, 2.00% Cr and 0.20% Mo, and 1.00% Ni was used as workpiece material. The application of this material is also used to produce plastic injection moulds; extrusion dies, blow moulds, tooling designs, and various other components measure 170 mm in length, 100 mm in width and 50 mm in height. The machining test was performed applying a cutting speed of v_c = 200 m/min, with a feed rate of f_z = 0.20 mm/tooth, a_e = 0.6 mm radial depth of the cut and a_p = 1.0 mm axial depth of the cut.

During the milling test, the cutting tool insert was periodically removed from the tool holder, and the flank wear on the flank face was measured using a Mitutoyo toolmakers microscope. The measured parameter representing the progress of wear was VB, being the average flank wear land. Six machining signals (F_c-F_t-F_{cN}-T_q-A_z-T_m) were collected simultaneously using the developed sensor system, and all data were recorded using the developed GUI at a sampling rate of 5 kHz.

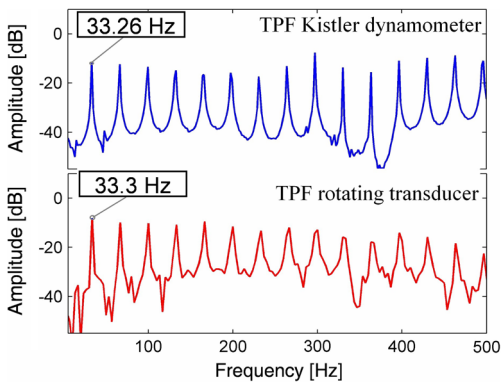

Fig. 14 Comparison of tool passing frequency of F_x and F_c when milling FCD700 at exp. set 1

4 Results and discussion

4.1 Calibration results

The calibration results of the torque sensor based on the strain gauges are shown in Fig. 9. It can be observed that the ratio of the torque voltage obtained using linear regression was 1.396 μV/Nm, which is, in theory, the sensitivity of the developed torque sensor. The same can be observed in Fig. 10, which shows the result of the temperature sensor calibration using a type-K thermocouple. The graph illustrates that the

Table 2 The results of comparison between developed force transducer and Kistler dynamometer

No. Exp.	Active force, F_a (N)		Error (%)	Force in z-axis (N)		Error (%)	Torque (T_q and M_z)(Nm)		Error (%)
	Rotating dynamometer	Kistler dynamometer		Rotating dynamometer	Kistler dynamometer		Rotating dynamometer	Kistler dynamometer	
Set 1	687	761	9.7	66	62	6.5	48	45	6.7
Set 2	915	983	6.9	73	80	8.8	54	53	1.9
Set 3	662	724	8.6	57	63	9.5	46	49	6.1
Set 4	779	885	12.0	63	73	13.7	47	52	9.6
Set 5	520	562	7.5	53	59	10.2	28	30	6.7
Set 6	651	747	12.9	60	68	11.8	36	41	12.2
Average error			9.6	Average error		7.9	Average error		7.2

temperature voltage ratio obtained using linear regression was 0.173 μV/°C.

4.2 Verification results

The comparative results from the cutting force signal in the time domain that was achieved using a 9257B Kistler dynamometer and a developed rotating transducer are shown in Figs. 11 and 12. It is evident that the patterns of the cutting force readings for both methods are similar, although they are different in the force value due to the varying orientation direction of the coordinate systems, namely fixed and rotating coordinates. However, the thrust force on the rotating transducer can be compared directly to the cutting force in the z-axis on a Kistler dynamometer, as shown in Fig. 13. The obtained average of the thrust force F_t was about 65 N, while the axial force F_z was about 67 N. The result indicates that the difference is not significant. In the frequency domain, it can be concluded that the frequency of the cutting tool (*tool passing frequency*—TPF) showed comparable results at about 33.3 Hz as illustrated in the frequency plot shown in Fig. 14. This, therefore, means that the developed rotating transducer provided a similar dynamic response reading compared to the Kistler dynamometer.

Figure 15 shows a time domain plot of the torque signal from a wireless sensor system based on using strain gauges and a moment signal in the z-axis from a Kistler dynamometer obtained during experimental set 1. This shows that the amplitude of the wireless torque signal after calibration was via the reading amplitude of the Kistler dynamometer. This result indicates that the reading of the developed torque sensor, based on strain gauges and using a wireless system, is reliable and can, therefore, be used to measure the torque in the milling process even during drilling. However, there is little interference in the readings of the torque signal caused by structural factors or tool holders, i.e. where the strain gauges are installed. This is inevitable due to the rotation of the tool holder, as well as the impact of the wireless devices on the tool holder during the milling process [20].

To compare the components of the main cutting force F_c and the perpendicular cutting force F_{cN} from the rotating force transducer to the cutting forces components of F_x and F_y on the Kistler dynamometer, Eq. (6) is applied to obtain the active force (F_a). A comparison is then made between the thrust

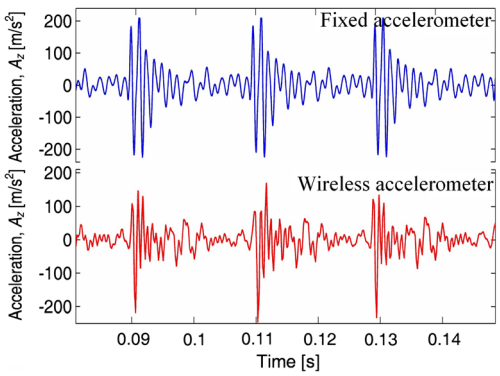

Fig. 16 Comparison of vibration signals in time domain of wireless and fixed sensors

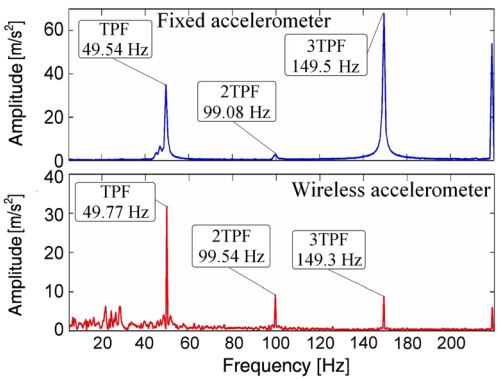

Fig. 17 Comparison of vibration signals in frequency domain of wireless and fixed sensors

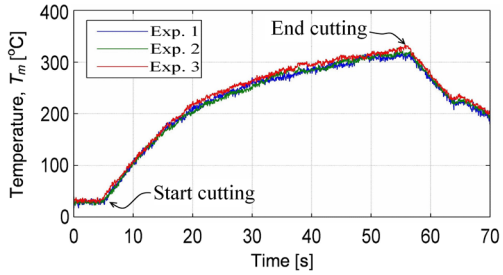

Fig. 18 Plot the temperature signal when milling cast iron

force on the rotating force transducer and the *z*-axis of the table dynamometer. The moment signal in the *z*-axis of the table dynamometer can be compared directly to the torque signal generated by the wireless torque sensor. The resultant errors of comparisons for some combinations of the experimental sets are shown in Table 2. The percentage error from the dynamometer readings indicates less than 13.7%, meaning that the accuracy of the readings obtained in the various experimental sets is almost like the readings from the existing commercial dynamometer. The average error of the dynamometer for the active force did not exceed 9.6%, while the average error of the cutting force in the *z*-axis is 7.9% and the average error of the torque or the moment is 7.2%. This relative error exhibits similar results to those in the comparative study of the force-based sensing system and the Kistler dynamometer [15, 21].

Figure 16 shows the vibration signal in the time domain obtained from experimental validation for experimental set 3. The graph plots the vibration of the fixed accelerometer on the rotating tool holder and a wireless accelerometer attached to the machine's structure. The figure also shows the apparent peak signal of vibration in the time domain indicating each rotation of the tool when cut and not cut. The vibration signals are also plotted in the graph of the frequency spectrum or cutting tool (tool passing frequency—TPF) as shown in Fig. 17.

Vibrations are generated by the interaction between the tool and the workpiece having frequency characteristics in multiples of the tool passing frequency of 1×, 2×, 3×, …62× [22]. This means that the signal in the time domain consists of a series of impulse-like peaks, causing integer multiples of its harmonics. The sharpness of the force impulses influences the relative magnitudes of these harmonics. As shown in Fig. 17, the frequency of the cutting tool is initially generated at 49.77 Hz. This is an accurate result, calculated, at a 2986-rpm rotation speed of the cutting tool, resulting in a frequency of 49.76 Hz. When compared to the amplitude of the frequency for both readings, it seems that the second TPF of the accelerometer placed on the machine structure appears small. By locating the accelerometer away from the cutting zone, damping effects are experienced in the structural spindle and bearings with this result being consistent with previous studies reporting that the signal quality is dependent primarily on the placement of the vibration sensors and vibration source [11, 23].

The resultant temperature readings obtained from the wireless thermocouple during the milling process are shown in Fig. 18. It is quite noticeable that during the milling test, the temperature attained while cutting workpieces of 170 mm in

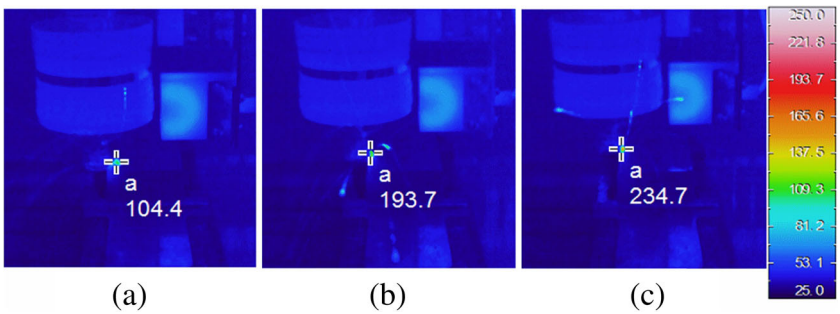

Fig. 19 Temperature spectrum from infrared camera at **a** 10, **b** 20 and **c** 30 s

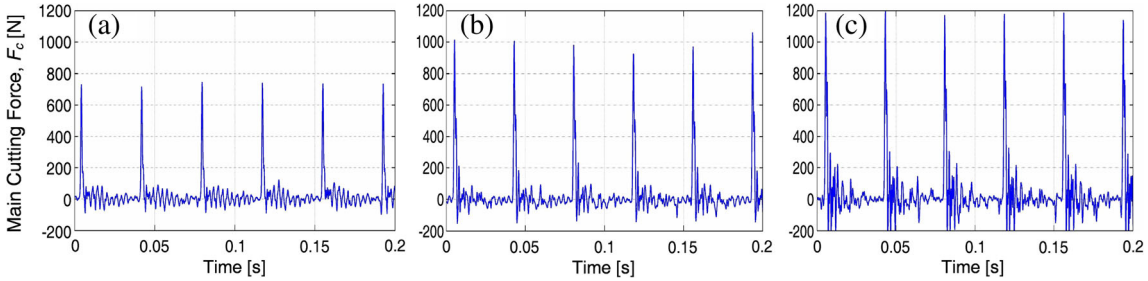

Fig. 20 Changes of main cutting force signal, F_c, in the time domain in three stages of tool condition. **a** $VB = 0$ mm. **b** $VB = 0.168$ mm. **c** $VB = 0.311$ mm

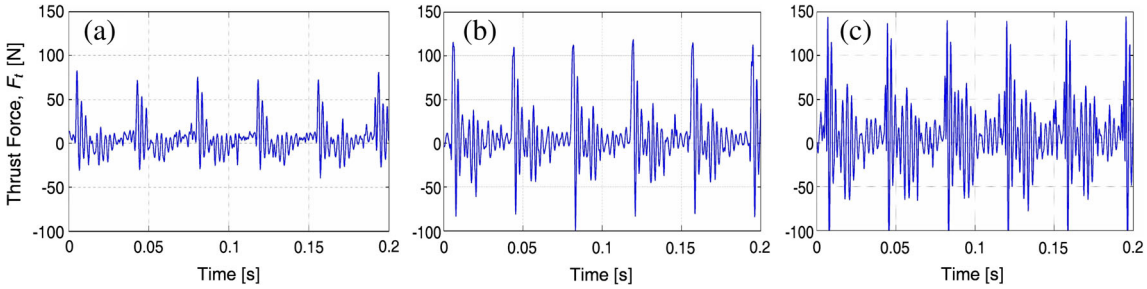

Fig. 21 Changes of thrust force signal, F_t, in the time domain in three stages of tool condition. **a** VB = 0 mm. **b** VB = 0.168 mm. **c** VB = 0.311 mm

length was about 320 °C, further showing that the temperature of the workpiece in and out of the zone of the cutting tool is not in a constant state. The temperature increased gradually along the cutting zone. This finding is in agreement with the results obtained by previous researchers [13, 14], which concluded that the temperature along the cutting zone increases gradually, with no fixed temperature attained.

From the temperature readings observed in Fig. 19, it may be said that the temperature readings for all three machining tests were very similar. The repeatability error of the thermocouple reading is within the range of 0.24 to 2.79%, which means that the thermocouple sensor used in this research provides a consistent reading. Also, the performance of the wireless temperature sensor system was tested by comparing temperature readings via an infrared camera NEC G100EX. Figure 20 shows the maximum temperatures observed on the edge of the tool at 10, 20 and 30 s, and 104.4, 193.7 and 234.7 °C, respectively. These results are dissimilar to that of the readings of the thermocouple wireless system's temperature recording during the same time intervals, which were 109, 213 and 251 °C, respectively. This indicates that the sensor system is reliable with satisfactory performance with an average variance of about 7.11%. This error is relatively small as compared with previous research reports which showed the percentage error was about 14% [14].

4.3 Machining test for tool condition monitoring

Actual experimental machining was carried out in CNC milling to assess the performance of a wirelessly integrated multisensor on a rotating cutting tool for tool condition monitoring. Figures 20, 21, 22, 23, 24 and 25 show the results of the six channels of machining signals recorded during the milling of AISI P20 + Ni tool steel. This was undertaken using a parameter machining cutting speed of v_c = 200 m/min, feed rate f_z = 0.2 mm/tooth, radial depth of cut a_e = 0.6 mm and an axial depth of cut a_p = 1.0 mm.

Figure 20 illustrates the main cutting force signal F_c, as well as the interval time between the peaks where the cutting tool was not touching or cutting the workpiece. It is clear that the cutting tool flank wear caused the main cutting force to increase. When initiating the milling process with the new tool or VB = 0 mm, the maximum amplitude of the force F_c was 738 N. As a result of the occurrence of flank wear VB = 0.168 mm, the peak reading of the main cutting force increased until reaching an amplitude of 994 N.

The amplitude continued to increase, such that at flank wear VB = 0.311 mm, the peak reading of F_c reached 1182 N. This indicated that the increase in the average force F_c due to the flank wear was 26.8%. This result is in agreement with the result as reported by Kuljanic and Sortino [24], which measured the force F_c using a rotating Kistler dyna-

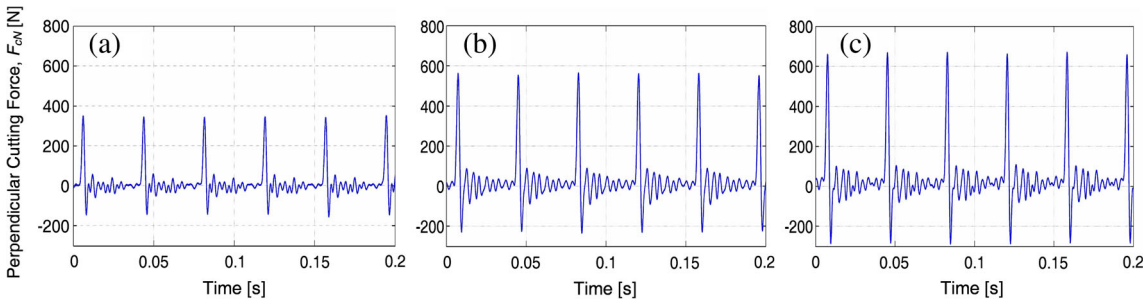

Fig. 22 Changes of perpendicular cutting force signal F_{cN} in the time domain in three stages of tool condition. **a** VB = 0 mm. **b** VB = 0.168 mm. **c** VB = 0.311 mm

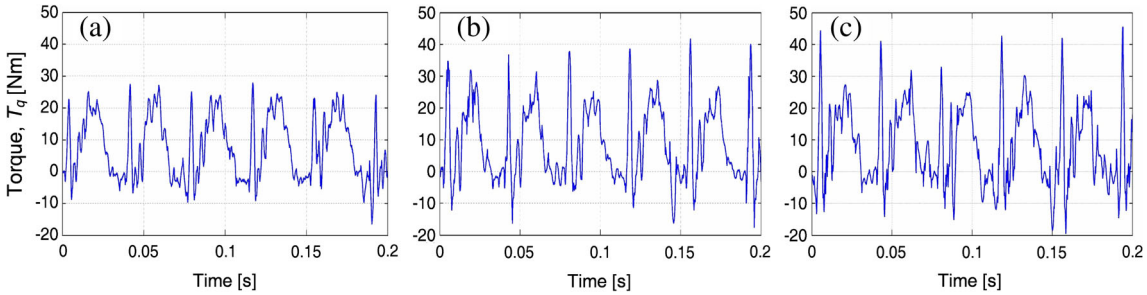

Fig. 23 Changes of torque signal T_q in the time domain in three stages of tool condition. **a** VB = 0 mm. **b** VB = 0.168 mm. **c** VB = 0.311 mm

mometer and observing an increase of around 20–22% in the main cutting force F_c due to flank wear.

Figure 21 shows the thrust force signal F_t in the time domain. Thrust force can be referred to as passive force. Furthermore, it was observed that the amplitude achieved was smaller than the main cutting force F_c due to the thrust force generated by the reaction of the work piece against the pressure of the cutting tool in the vertical direction [25]. Moreover, the amplitude of the thrust force F_t showed a reading of only 70 N in the initial cutting process (VB = 0 mm). However, thrust force F_t was also sensitive to changes in tool flank wear. When the flank wear reached VB = 0.168 mm, the amplitude was 116 N, increasing up to an amplitude of 143 N at flank wear VB = 0.311 mm. Thus, the average increase in the amplitude of the thrust force F_t was 44.5%.

The result of the perpendicular cutting force signal F_{cN} is plotted in the graph as shown in Fig. 22. The changes in the force F_{cN} amplitude are due to the significant increase of the flank wear. For instance, when cutting using a new tool (VB = 0 mm), the amplitude of the force F_{cN} was 338 N.

Likewise, when cutting continued and reached the flank wear VB = 0.168 mm, the amplitude of the force also increased to 513 N. Furthermore, at the flank wear VB = 0.311 mm, the amplitude readings peaked at 645 N. Subsequently, the average increase in the amplitude force signal F_{cN} was 38.7%. These results indicate that the perpendicular cutting force signal F_{cN} has high sensitivity to changes in flank wear. These results are consistent with the results obtained by Kuljanic and Sortino [24].

Figure 23 shows the amplitude changes of the torque signal caused by the progression of tool flank wear. During the initial milling with the sharp tool, the torque reading reached to about 22 Nm. However, when the flank wear started to increase at 0.168 mm, there was a corollary 34 Nm increase in the torque readings. Similarly, there was a progressive rise in the readings until about 42 N at the flank wear value VB = 0.311 mm. This illustrates that torque signals have an important relationship with changes in flank wear. These results are in agreement with prior studies, which measured the torque using a torque-based sensorised tool holder [26] or based on a rotating dynamometer [27].

The results relating to the vibration signals in the time domain on the three stages of flank wear are shown in Fig. 24. The increase in the amplitude of the vibration in the raw signal was insignificant when there was a change in the flank wear value. However, observing the pattern of the peak-to-peak signals closely revealed signal pattern changes due to flank wear. The resulting crest-of-waves pattern at any one period, for an increase in the number (i.e. value), indicated frequency increases. Also, the vibration signals had a significant relationship with the change in flank wear, normally analysed using feature extraction methods in the frequency domain [22, 28].

Figure 25 shows the changes in the temperature signal readings due to tool flank wear in the time domain, indicating

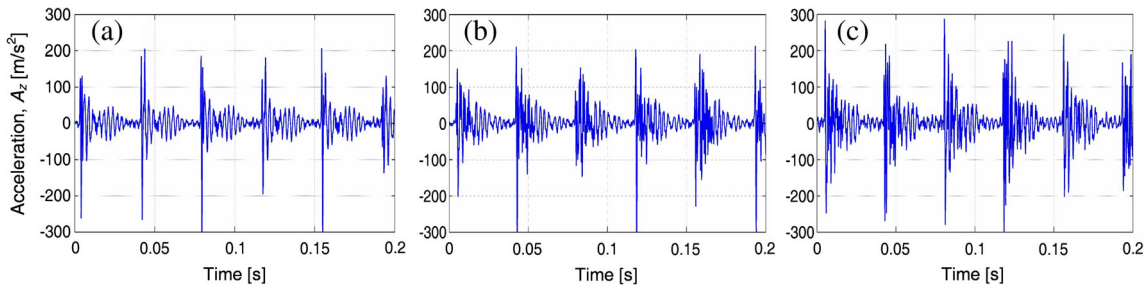

Fig. 24 Changes of vibration signal, A_z, in the time domain in three stages of tool condition. **a** VB = 0 mm. **b** VB = 0.168 mm. **c** VB = 0.311 mm

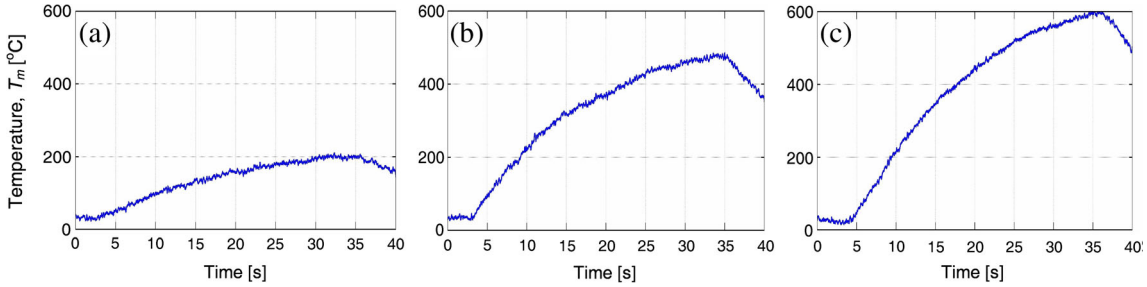

Fig. 25 Changes of temperature signal, T_m, in the time domain in three stages of tool condition. **a** VB = 0 mm. **b** VB = 0.168 mm. **c** VB = 0.311 mm

that the flank wear of the tool caused the rate of temperature to increase, caused by the rubbing action between the flank edge of the cutting tool and the surface of the work piece [29].

All six results relating to the main cutting force, thrust force, perpendicular cutting force, torque, vibration and temperature found that the developed wireless integrated multi-sensor is highly sensitive but effective to the changing progression of flank wear. This statement is supported by prior experiments that measured the cutting forces and torque to monitor the tool using a rotating dynamometer [24, 26] or table dynamometer [27], a vibration signal [22] and temperature [30]. Therefore, this sensor system is suitable for real-time tool condition monitoring during the milling process.

5 Conclusion

This paper proposed a new wireless integrated multi-sensor on rotating tools for real-time tool condition monitoring in the milling process. The sensor system is capable of simultaneously measuring the six channels of machining signals: the main cutting force, perpendicular cutting force, thrust force, torque, vibration and temperature. Furthermore, the system provides for flexible and re-configurable cutting tools since it is interchangeable and compatible with distinct standard modules.

The calibration, verification and real experimental machining tests were undertaken to evaluate the performance of the developed sensor system with the results highlighting the following outcomes:

- The sensitivities of torque and temperature sensors (T_q and T_m) were 1396 μV/Nm and 0.173 μV/°C.
- The verification results of the force transducer and torque sensor obtained an average error of less than 9.6% when compared to the existing dynamometer.
- The repeatability error of the wireless temperature sensor was in the range of 0.24 to 2.79%, while the average relative error was about 7.11% when compared to the infrared camera readings.
- The six channels of machining signals have significant correlation with the progression of flank wear.
- The prototype of the new wireless integrated multi-sensor is reliable and can be utilised for studies on cutting processes, optimisation and real-time tool condition monitoring systems.

Funding information The authors wish to thank the Government of Malaysia (MOSTI) through Universiti Kebangsaan Malaysia (UKM) for their financial support under Grant 03-01-02-SF0843 and the Ministry of Research, Technology and Higher Education of the Republic of Indonesia.

References

1. Rehorn AG, Jiang J, Orban PE (2005) State-of-the-art methods and results in tool condition monitoring: a review. Int J Adv Manuf Tecnol 26:693–710
2. Abellan-Nebot JV, Subirón FR (2010) A review of machining monitoring systems based on artificial intelligence process models. Int J Adv Manuf Tecnol 47:237–257
3. Teti R, Jemielniak K, O'Donnell G, Dornfeld D (2010) Advanced monitoring of machining operations. CIRP Annals - Manuf Technol 59:717–739
4. Sick B (2002) On-line and indirect tool wear monitoring in turning with artificial neural networks: a review of more than a decade of research. Mech Syst Signal Process 16(4):487–546
5. Korkut I (2003) A dynamometer design and its construction for milling operation. Mater Des 24:631–637
6. Yaldız S, Unsacar F, Saglam H, Isık H (2007) Design, development and testing of a four-component milling dynamometer for the measurement of cutting force and torque. Mech Syst Signal Process 21: 1499–1511
7. Oliveira JFG, Valente CMO (2004) Fast grinding process control with AE modulated power signals. CIRP Annals - Manuf Technol 53(1):267–270
8. Shao H, Shi X, Li L (2011) Power signal separation in milling process based on wavelet transform and independent component analysis. Int J Mach Tools Manuf 51:701–710
9. Shi X, Wang R, Chen Q, Shao H (2014) Cutting sound signal processing for tool breakage detection in face milling based on empirical mode decomposition and independent component analysis. J Vib Control doi. https://doi.org/10.1177/1077546314522826
10. Kalvoda T, Hwang Y-R (2010) A cutter tool monitoring in machining process using Hilbert–Huang transform. Int J Mach Tools Manuf 50:495–501
11. O'Donnell G, Young P, Kelly K, Byrne G (2001) Towards the improvement of tool condition monitoring systems in the manufacturing environment. J Mater Process Technol 119(1–3): 133–139

12. Suprock CA, Fussell BK, Hassan RZ, Jerard RB A low cost wireless tool tip vibration sensor for milling. In: ASME (ed) The International Manufacturing Science and Engineering Conference (MSEC2008), Evanston, IL, USA, 7–10 October 2008 2008. ASME, pp 1–10
13. Coz GL, Marinescu M, Devillez A, Dudzinski D, Velnom L (2012) Measuring temperature of rotating cutting tools: application to MQL drilling and dry milling of aerospace alloys. Appl Therm Eng 36:434–441
14. Kerrigan K, Thil J, Hewison R, O'Donnell GE (2012) An integrated telemetric thermocouple sensor for process monitoring of CFRP milling operations. Procedia CIRP 1:449–454
15. Totis G, Wirtz G, Sortino M, Veselovac D, Kuljanic E, Klocke F (2010) Development of a dynamometer for measuring individual cutting edge forces in face milling. Mech Syst Signal Process 24: 1844–1857
16. Ma L, Melkote SN, Castle JB (2014) PVDF sensor-based monitoring of milling torque. Int J Adv Manuf Tecnol 70(9–12):1603–1614
17. Rizal M, Ghani JA, Nuawi MZ, Haron CHC (2015) Development and testing of an integrated rotating dynamometer on tool holder for milling process. Mech Syst Signal Process 52-53:559–576
18. Qin Y, Zhao Y, Li Y, Zhao Y, Wang P (2017) A novel dynamometer for monitoring milling process. Int J Adv Manuf Tecnol DOI. https://doi.org/10.1007/s00170-017-0292-3:1-9
19. Xie Z, Lu Y, Li J (2017) Development and testing of an integrated smart tool holder for four-component cutting force measurement. Mech Syst Signal Process 93:225–240
20. Suprock CA, Nichols JS (2009) A low cost wireless high bandwidth transmitter for sensor-integrated metal cutting tools and process monitoring. Inter J Mechatron Manuf Sys:441–454
21. Ma L, Melkote SN, Morehouse JB, Castle JB, Fonda JW (2010) On-line monitoring of end milling forces using a thin film based wireless sensor module. In: ASME (ed) Proceedings of the ASME International manufacturing science and engineering conference, Erie, Pennsylvania, USA, October 12–15, 2010 2010. ASME,
22. Orhan S, Er AO, Camuscu N, Aslan E (2007) Tool wear evaluation by vibration analysis during end milling of AISI D3 cold work tool steel with 35 HRC hardness. NDT&E International 40(2):121–126
23. Haber RE, Jiménez JE, Peres CR, Alique JR (2004) An investigation of tool-wear monitoring in a high-speed machining process. Sens Actuators, A 116(3):539–545
24. Kuljanic E, Sortino M (2005) TWEM, a method based on cutting forces—monitoring tool wear in face milling. Int J Mach Tools Manuf 45:29–34
25. Schulze V, Becke C, Weidenmann K, Dietrich S (2011) Machining strategies for hole making in composites with minimal workpiece damage by directing the process forces inwards. J Mater Process Technol 211(3):329–338
26. Dini G, Tognazzi F (2007) Tool condition monitoring in end milling using a torque-based sensorized toolholder. Proc Inst Mech Eng Part B J Eng Manuf 221:11–23
27. Kaya B, Oysu C, Ertunc HM (2011) Force-torque based on-line tool wear estimation system for CNC milling of Inconel 718 using neural networks. Adv Eng Softw 42:76–84
28. Rizal M, Ghani JA, Nuawi MZ, Haron CHC (2014) A wireless system and embedded sensors on spindle rotating tool for condition monitoring. Adv Sci Lett 20(10–12):1829–1832
29. Lin S, Peng F, Wen J, Liu Y, Yan R (2013) An investigation of workpiece temperature variation in end milling considering flank rubbing effect. Int J Mach Tools Manuf 73:71–86
30. Choudhury SK, Bartarya G (2003) Role of temperature and surface finish in predicting tool wear using neural network and design of experiments. Int J Mach Tools Manuf 43(7):747–753